

## Limits to the quantification of local climate change

This content has been downloaded from IOPscience. Please scroll down to see the full text.

2015 Environ. Res. Lett. 10 094018

(<http://iopscience.iop.org/1748-9326/10/9/094018>)

View [the table of contents for this issue](#), or go to the [journal homepage](#) for more

Download details:

IP Address: 129.242.167.242

This content was downloaded on 01/03/2016 at 12:39

Please note that [terms and conditions apply](#).



## LETTER

## Limits to the quantification of local climate change

## OPEN ACCESS

RECEIVED  
28 May 2015

REVISED  
15 July 2015

ACCEPTED FOR PUBLICATION  
16 July 2015

PUBLISHED  
16 September 2015

Content from this work  
may be used under the  
terms of the [Creative  
Commons Attribution 3.0  
licence](#).

Any further distribution of  
this work must maintain  
attribution to the  
author(s) and the title of  
the work, journal citation  
and DOI.



Sandra C Chapman<sup>1,4</sup>, David A Stainforth<sup>2,1,3,5</sup> and Nicholas W Watkins<sup>3,1</sup>

<sup>1</sup> Department of Physics, University of Warwick, Coventry, CV4 7AL, UK

<sup>2</sup> Grantham Research Institute on Climate Change and the Environment, Houghton Street, London, UK

<sup>3</sup> Centre for the Analysis of Timeseries, London School of Economics, Houghton Street, London, UK

<sup>4</sup> Department of Mathematics and Statistics, University of Tromsø, N-9037 Tromsø, Norway

<sup>5</sup> Environmental Change Institute, University of Oxford, Oxford OX13QY, UK

E-mail: [S.C.Chapman@warwick.ac.uk](mailto:S.C.Chapman@warwick.ac.uk)

**Keywords:** climate change, precipitation, climate change uncertainties

Supplementary material for this article is available [online](#)

### Abstract

We demonstrate how the fundamental timescales of anthropogenic climate change limit the identification of societally relevant aspects of changes in precipitation. We show that it is nevertheless possible to extract, solely from observations, some confident quantified assessments of change at certain thresholds and locations. Maps of such changes, for a variety of hydrologically-relevant, threshold-dependent metrics, are presented. In places in Scotland, for instance, the total precipitation on heavy rainfall days in winter has increased by more than 50%, but only in some locations has this been accompanied by a substantial increase in total seasonal precipitation; an important distinction for water and land management. These results are important for the presentation of scientific data by climate services, as a benchmark requirement for models which are used to provide projections on local scales, and for process-based climate and impacts research to understand local modulation of synoptic and global scale climate. They are a critical foundation for adaptation planning and for the scientific provision of locally relevant information about future climate.

## 1. Introduction

The focus of climate change science and policy has shifted from global to local. Local changes, particularly in extremes and at user-specific thresholds, influence both practical planning [1–4] (adaptation) and individuals' perceptions, which ultimately drive mitigation policy. The much discussed hiatus [5] in global mean temperature adds urgency to today's core challenge of climate science; to understand how global change arises from and drives changes at small spatial scales. A key starting point is to quantify the observed changes in distribution. Some robust aspects of observed changes in local temperature distributions have been identified [6, 7], but precipitation raises significantly greater challenges because our interests are in the tails of what are often heavier-tailed (leptokurtic) distributions, and user requirements demand flexible approaches which quantify different types of hydrological vulnerability and address local factors.

Establishing the connection between changing climate at global scales and its consequences at local scales is key for the scientific underpinning of adaptation policy and strategic development initiatives, as well as for public and policy debates about climate change. From a research perspective, understanding the way meso-scale climate alters in response to changes in local, distant and global forcing, and long term variations in synoptic patterns, is a critical element of climate change science. Such research must acknowledge that climate change is a change in distribution [6–8]. For temperature variables some studies have extracted distributional information from observations [9] and from a combination of models and observations [10, 11]. Such studies have achieved resolution in distribution at the cost of reliable local detail, either through assuming spatial correlations or as a consequence of limits to the fine scale interpretation of models [12–15]. Non-parametric, non-model-based analyses have identified some robust aspects of

observed changes in local temperature distributions [6, 7] but it has been an open question whether such approaches could be applied to precipitation.

Sub-continental scale assessments of observed changes have traditionally focused on mean changes [16] although in recent years the emphasis has shifted to extremes [17]. A range of indices have been developed [18, 19] which focus on high percentiles (e.g. rainfall falling on days above the 99th percentile) and on absolute extremes (e.g. maximum annual one day precipitation) but scientific assessments are best undertaken in the context of changes in the whole climatic distribution [6–8]. Furthermore, climate-vulnerable policy decisions, adaptation planning and impact assessments all have different relevant thresholds and sensitivities. Here we utilize a methodology which maintains the flexibility to provide information at different thresholds for different downstream users; both scientists and decision makers.

While previous studies have analysed changes in regional and local precipitation distributions within models [20], often using dynamical or statistical downscaling, the interpretation of model assessments such as CMIP5 [21] must account for the degree to which such models can reproduce the observed local changes in distribution. Whether ones aim is to quantify and understand observed changes directly, or to interpret models in terms of real world behaviour, a key question is therefore: to what extent can changes in local climatic distributions be quantified given the limited length timeseries available? To answer this question we begin in section 2 by demonstrating the implications of unavoidable data constraints, using idealized parametric precipitation distributions. European local precipitation timeseries are then analysed in section 3 in the light of such constraints using a non-parametric approach. Finally in section 4, maps of observed changes are presented which reveal spatially extended patterns of threshold dependent changes. This spatial coherence is interpreted as an additional source of confidence in the identified character of (unattributed) local climate change.

## 2. Fundamental data constraints

To demonstrate the challenges in observational interpretation, daily precipitation in a season is first taken to be drawn randomly from a gamma distribution [20, 22, 23] (see appendix). Climate change is represented by changes in the parameters of the distribution over a 63 year period leading to distributions with (i) no change over time, (ii) increasing mean, (iii) increasing mean, variance, skew and kurtosis, and (iv) increasing variance, skew and kurtosis but no change in mean (figures 1(o), (e), (f)). Climate change is then quantified by changes between distributions separated by a 45 year period (see appendix). In evaluating the change in distribution we use four threshold ( $T$ )

dependent quantities, herein referred to as climate change descriptors: (a) change in quantile,  $\Delta Q_T$ , which reflects a change in the rain intensity one would expect to exceed with a particular frequency [6, 24], (b) change in total seasonal precipitation above a threshold  $\Delta \Sigma P_T$ , (c) change in total seasonal precipitation above a threshold as a percentage of the historical average, relative  $\Delta \Sigma P_T$ , and (d) change in the fraction of total seasonal precipitation that falls on days wetter than the threshold,  $\Delta F_T$ . Each descriptor reflects different aspects of the changing distribution; aspects which affect different decisions, vulnerabilities and climatological/hydrological process research. Their presentation as a function of threshold represents a generalization of conventional climate change indices [18, 19].

In this idealized case the underlying distributions are known and the climate change descriptors can be accurately quantified by well sampling them in each year (see appendix). In figures 1(a)–(d) the solid yellow lines illustrate this situation of almost perfect knowledge. In this case the results represent a precipitation-relevant extension of the common illustration of climate change in terms of a Gaussian distribution subject to increasing mean and/or variance [17] (see also SI figure 1).

The nature of the real-world system, however, provides data limitations which restrict what we can know about such quantities from observations. Studying daily precipitation during a season limits the available data to approximately 90 samples/year from the underlying distribution. Samples from multiple years can be combined (the commonly-made kairoic assumption, e.g. [8]) but if changes are believed to be occurring on a decadal timescale, as they are under anthropogenic climate change, then conflating data from more than a handful of years suppresses the signal of interest. A balance must therefore be struck between sampling resolution, the period over which changes are assessed and the ability to explore uncertainty. In figure 1, data over blocks of nine successive years is aggregated to represent each year [6] (see appendix). The distributions are nevertheless still of limited resolution but multiple evaluations over different overlapping 45 year periods within a single timeseries can be made and these are plotted as thin coloured (blue through magenta) lines on figures 1(a)–(d). Taken together they demonstrate the considerable uncertainty in data-derived conclusions regarding the climate change descriptors.

Under no change over time the well-sampled distributions (bold yellow lines) demonstrate the trivial conclusion that all the metrics are zero for all thresholds, but variations in their estimates when data is constrained are large (figure 1(i)). Furthermore, because the different estimates of change come from a single timeseries they are not independent. This increases the likelihood of substantial biases across all estimates (see for instance figures 1(i), (b)). There is therefore no

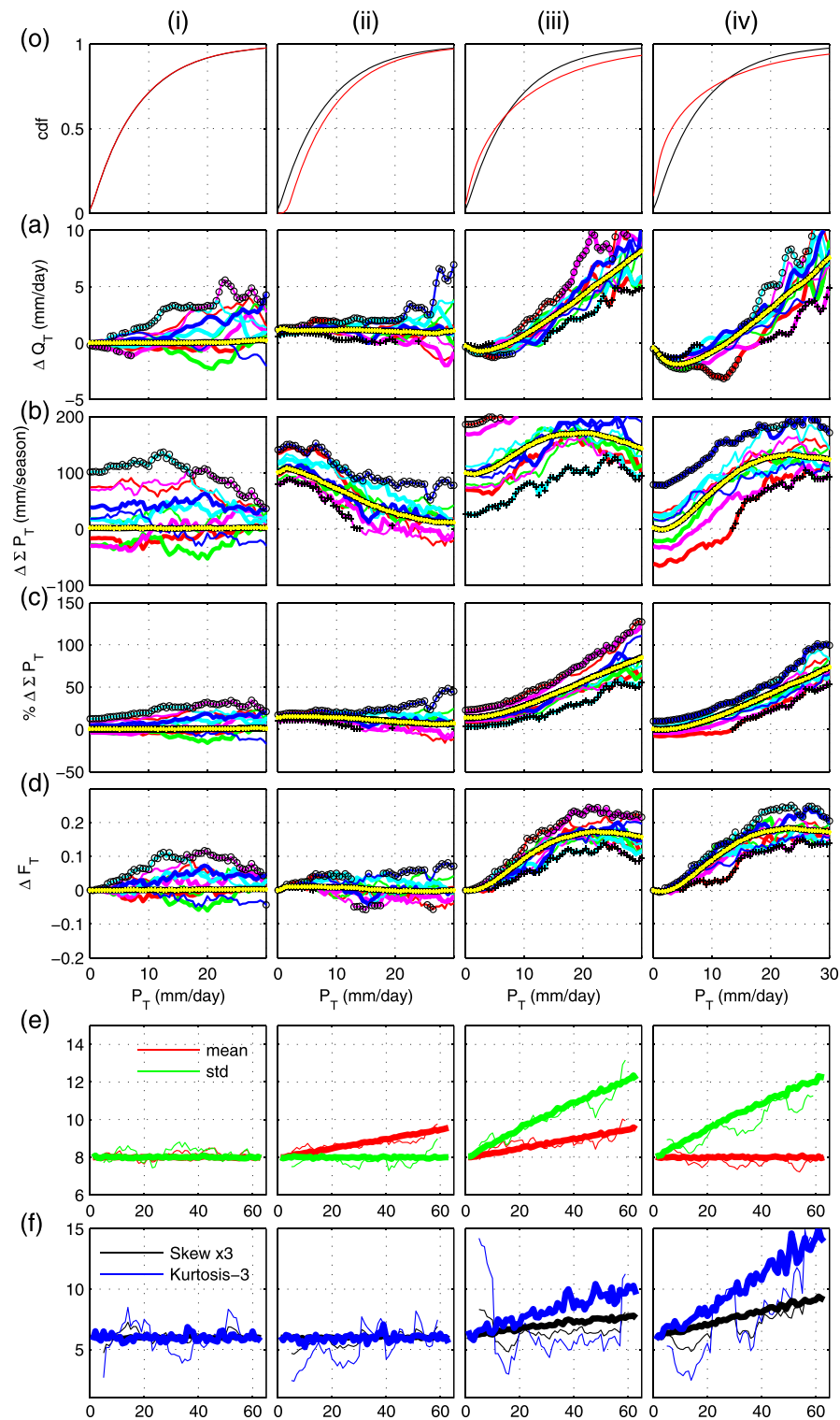


**Figure 1.** Idealized climate change with limited data and with almost perfect knowledge. (o) Cumulative distribution functions at the beginning (black) and end (red) of the illustrative 63 year period for (i) a constant distribution, (ii) increasing mean only, (iii) increasing mean, variance, skew and kurtosis, and (iv) increasing variance, skew and kurtosis. (a) Solid lines coloured blue through magenta plot ten samples of change in quantile,  $\Delta Q_T$ , over moving 45 year periods (from the middle of season within year 5 to the middle of the same season within year 50, 6 to 51, ..., 14 to 59) within the 63 year timeseries, where each year's distribution is represented by 9 years of data (for year  $t$  this includes years  $t - 4$  to  $t + 4$ —see appendix) and each year contains 90 samples from its underlying distribution. This is analogous to looking at a real-world timeseries built from one season/year. The bold yellow line shows the change between years 9 and 54 (a central sample) but taking each year's distribution as represented by 100 000 samples from its underlying distribution—also see SI figure 1. Rows (b), (c), and (d), are as (a) but for the climate change descriptors: (b)  $\Delta \Sigma P_T$ , (c) relative  $\Delta \Sigma P_T$ , and (d)  $\Delta F_T$ . Plots (o)–(d) are functions of daily precipitation threshold ( $P_T$ ). Largest and smallest changes of consistent sign (see appendix) are marked with circles and crosses respectively. Rows (e) and (f) show the time-dependence of the mean (red), standard deviation (green), skew (black) and kurtosis (blue) for the well-sampled case (bold lines) and the realistically sampled case (standard lines).

justification for statistically combining them into a mean or probabilistic estimate. In real world time-series, long period oscillations (e.g. North Atlantic Oscillation, Pacific Decadal Oscillation etc) create inter-annual dependencies which reinforce this problem. Consequently the most relevant aspects are the largest, smallest and range of change at any particular threshold [7, 25] (see appendix), with the smallest change (when all estimates are consistent in sign) representing a conservative measure of identifiable change (figures 1(a)–(d), crosses). Some aspects of the signal of change can be identified despite these constraints.

Even in this highly idealized situation the picture is complicated. Details of both the underlying changes and their identifiability are in the supplementary discussion, but two features stand out. First, for changes above mid- to high thresholds, changes in higher moments are of far greater significance than changes in the mean, although changes in the mean can strongly influence identifiability. Second, conclusions are hampered by fundamental limits to data but indications of the underlying changes are nevertheless sometimes identifiable.

### 3. European local precipitation timeseries

The idealized analysis suggests that observational timeseries alone may reveal valuable information but that accurate quantification of the underlying changing full distribution is unlikely to be possible. Figure 2 demonstrates that this is indeed the case. Using the E-Obs [26] dataset, it shows that in South–West Scotland (figure 2(i)) total winter precipitation has increased and that relative  $\Delta\Sigma P_T$  is greater for higher thresholds up to  $\sim 25 \text{ mm d}^{-1}$  i.e. there is more overall precipitation and it is coming disproportionately more on heavy rainfall days. This contrasts with central Scotland (figure 2(ii)) where there is only a small identifiable increase in total precipitation but a shift of what there is towards heavier rainfall days. A very different response is seen in the Dordogne (figure 2(iii)) where there is an overall drying signal with a similar relative  $\Delta\Sigma P_T$  reduction across most thresholds. In all these cases the range of identified uncertainty in the response is relatively small and the signals discussed can be associated with the conservative, smallest-identified consistent response. This is, of course, not always the case. In South West Wales (figure 2(iv)) the range is not only large but includes zero; e.g. changes in total precipitation range from zero to  $100 \text{ mm d}^{-1}$  and remain broad across most thresholds. Here variability prevents any confident identification of threshold-dependent change over the period studied.

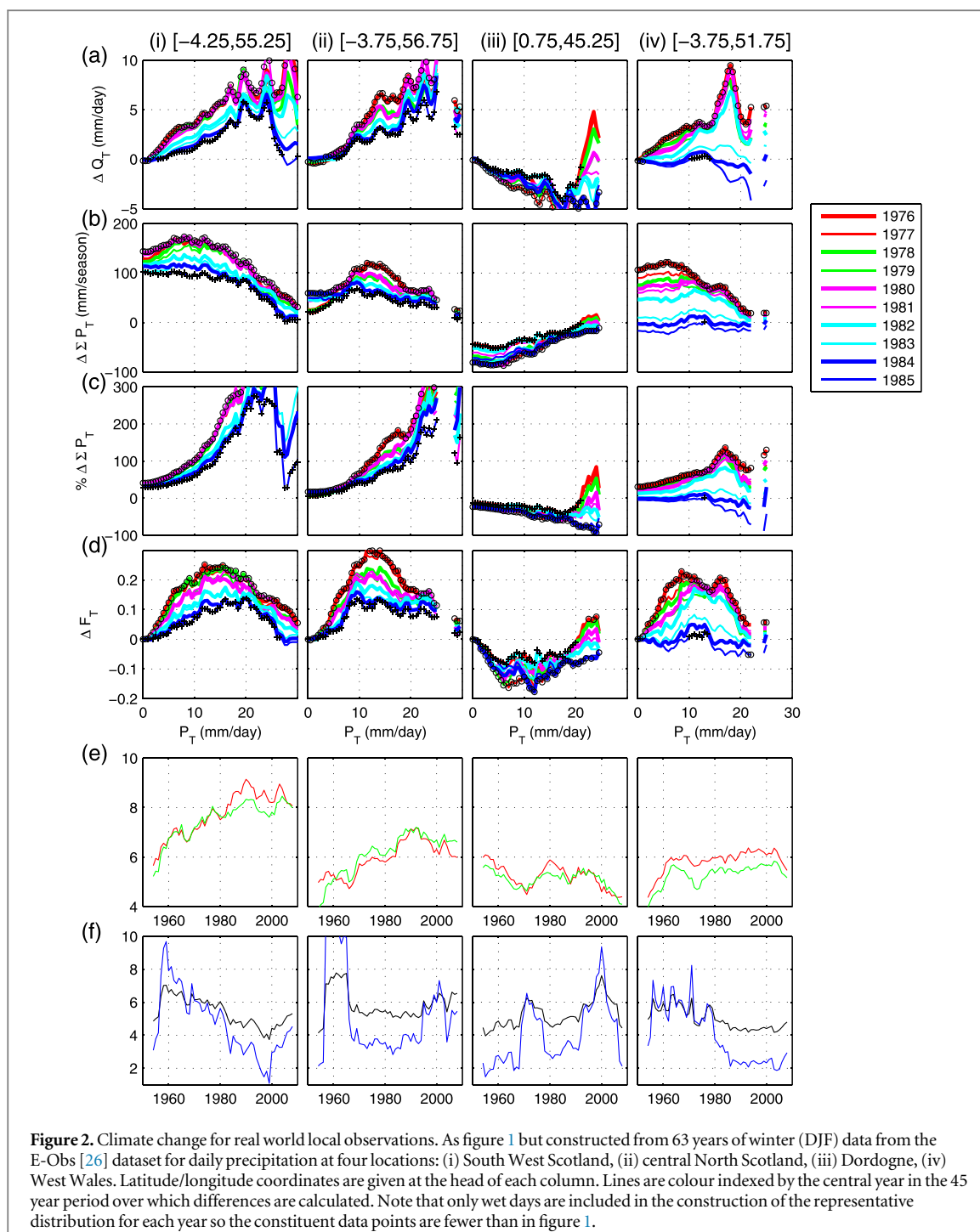
### 4. Maps of observed changes

Emergent spatial response patterns can provide increased confidence in identifiable signals, and coherent spatial patterns are found in the identifiable changes of all climate change descriptors (figure 3 and SI figure 3). In Scotland quantile changes are particularly large only at the highest quantiles, in South West France a pattern of decreases can be seen which is large for all quantiles above the 25th percentile, while across Northern Germany and the low countries a smaller but coherent pattern of increased precipitation stands out around the 75th percentile. Such variations illustrate the need to consider the whole distribution. Taking a series of fixed rainfall thresholds instead of quantile thresholds enables different aspects to be identified (figure 3(b) and SI figure 3). A reduction in rainfall amount in South West France can be seen in relative  $\Delta\Sigma P_T$  at all thresholds. The spatial extent of identifiable decline decreases at higher thresholds but the scale of decline does not, indicating that all intensities of rain are reducing in a similar fashion. This contrasts with the drying in central-Northern Italy which has greater reductions in days with particularly high rainfall, Scotland where increases are greatest in the heavier rainfall days, and Eastern Germany/Western Austria where increases are only identifiably large around the  $10 \text{ mm d}^{-1}$ , mid-range threshold. Many of these spatial patterns are also seen in the largest changes (SI figures 4 and 5).

### 5. Concluding remarks

These results highlight the complex and fine-scale patterns of changing climate, demonstrating that generic descriptions cannot capture relevant local characteristics and will inevitably jar with local perceptions. Global/synoptic scale climate change may sometimes be relatively easily identified but quantifying how this is reflected in (or built from) mesoscale/local changes faces intrinsic barriers. Yet such information is sought for societal planning and the analysis herein shows that in some regions the precipitation changes, like the temperature changes [7], have already been so significant as to be identifiable in distribution despite the variability and limited length timeseries available. Such information is of direct value in adaptation planning.

The results herein represent what might be termed ‘observations of climate change’, as opposed to raw observations of weather, and as such have a significant role to play in geophysical research on the meso-scale modulation of synoptic scale changes. Nascent climate services initiatives [27] could use such physical science to guide the conceptual exploration of future possibilities [28] and to evaluate the relevance and trustworthiness of model-derived projections, as well as providing observational data directly through the



automated processing of observations for specific user-relevant thresholds and vulnerabilities.

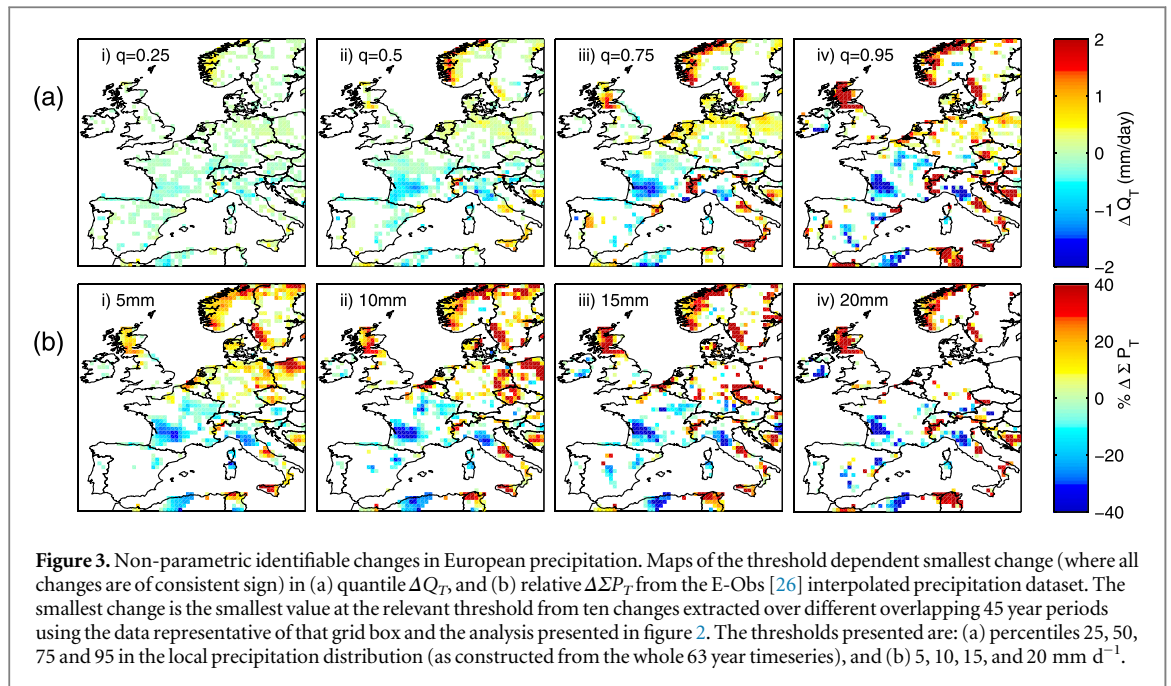
## Acknowledgments

We acknowledge the E-OBS dataset from the EU-FP6 project ENSEMBLES (<http://ensembles-eu.metoffice.com>) and the data providers in the EC&D project (<http://eca.knmi.nl>). DAS gratefully acknowledges the support of LSE's Grantham Research Institute on Climate Change and the Environment, the LSE's Centre for the Analysis of Timeseries, and the Centre for Climate Change Economics and Policy funded by

the Economic and Social Research Council and Munich Re. SCC and NWW acknowledge the Max Planck Institute for the Physics of Complex Systems visitor programme. We acknowledge EPSRC's CliMathNet and NetworkPlus EP/K000632/1, and KLI-MAFORSK 229754.

## Appendix

The analysis herein is founded on the processing of timeseries of daily precipitation at specific locations, over a 63 year period, using data from only one season in each year; in figures 2 and 3 this is the Boreal winter



—December/January/February (DJF)—during the period 1950–2012. Conceptually, the location specific daily precipitation is considered to be drawn from an underlying distribution representative of that season and year. The paper examines the ability to identify changes in decision relevant thresholds if this distribution is changing in time.

In the illustrative case (figure 1) the distribution is taken to be a gamma distribution with shape parameter  $k_t$  and scale parameter  $\theta_t$ , where  $t$  is the year index running from 1 to 63. In year zero  $k_1 = 1$ , and  $\theta_1 = 8$ . In figure 1, column (i) this distribution remains constant through the 63 years. In column (ii) the distribution is simply shifted so that the mean ( $k\theta$  for a gamma distribution) linearly increases by  $0.025 \text{ mm d}^{-1} \text{ yr}^{-1}$ . In column (iii),  $k_t$  monotonically decreases with time and  $\theta_t$  monotonically increases with time such that the mean linearly increases by  $0.025 \text{ mm d}^{-1} \text{ yr}^{-1}$  and the variance ( $k\theta^2$  for a gamma distribution) linearly increases by  $1.4 \text{ mm}^2 \text{ d}^{-2} \text{ yr}^{-1}$ . In column (iv),  $k_t$  monotonically decreases with time and  $\theta_t$  monotonically increases with time such that the mean stays constant and the variance linearly increases by  $1.4 \text{ mm}^2 \text{ d}^{-2} \text{ yr}^{-1}$ . The changes addressed in columns (iii) and (iv) both involve monotonically increasing skew and kurtosis. The resulting changes over time of all four moments are presented in figures 1(e), (f). These distributions are presented only for the purpose of illustration but the shape parameters of the gamma distributions fall within the domain of those found across Europe in the E-Obs dataset [26] (SI figure 2) throughout all the timeseries with the exception of the final few years of case (iv).

The bold lines in figures 1(a)–(d), and all the lines in SI figures 1(a)–(d), take the number of ‘days in a season’ to be 100 000 so that in each year the

distribution is well sampled. The thin coloured (blue through magenta) lines in figure 1 take the number of days in a season to be 90. This is similar to a real-world season but the resolution of the cumulative distribution function built from this number of points is too small for the subsequent analysis [6, 7]. Distributions taken to be representative of each year are therefore constructed using 9 years of data from year  $t-4$  to  $t+4$  inclusive. This means that samples from different distributions are combined into one, as they have to be in the analysis of real-world observations. The choice of 9 years has been shown in previous studies to provide a suitable compromise between increasing the resolution of the distribution and smoothing any changes in distribution over time [6, 7].

Changes in the climate descriptors are calculated from these annually representative distributions by taking differences over ten sample 45 year periods: years 5 to 50, 6 to 51 ... 14 to 59.  $\Delta Q_T$ , represents a change in quantile at constant cumulative probability [6, 24] e.g. if 95% of days have less than  $20 \text{ mm d}^{-1}$  but previously 95% had less than  $15 \text{ mm d}^{-1}$  then the change,  $\Delta Q_{0.95}$ , is  $5 \text{ mm d}^{-1}$ . In row (a) of figures 1 and 2, the daily rainfall thresholds are quantiles used to reflect the cumulative probability in the distribution constructed from all 63 years; in this example  $\Delta Q_{0.95}$  might therefore be associated with a rainfall threshold of approximately  $17.5 \text{ mm d}^{-1}$ . In figure 3 the maps are each for the same local cumulative probability.  $\Delta Q_T$  is calculated using the method of Chapman *et al* 2013 [6]. The remaining descriptors are calculated directly from the data taken to be representative of each year. Results are not plotted in figure 3 or SI figures 3–5 if the probability of occurrence at that threshold is less than  $0.001/(\text{mm d}^{-1})$ . In addition, results are not plotted in figure 3 and SI figure 3, if any

of the ten samples have different signs of change at the relevant threshold. This provides a first order indication of the insufficiency of the data for this analysis. We then consider the most informative aspects to be the largest change (the maximum absolute change—SI figures 4 and 5), the smallest change (taken to be zero if the samples have different signs, otherwise the minimum absolute change—figure 3 and SI figure 3) and the range (the difference between maximum change and minimum change). See Stainforth *et al* [7] for further discussion.

Figure 2 uses the same method as the thin lines in figure 1 but with DJF data from four grid boxes of the E-Obs version 10 dataset [26] which provides time-series of daily precipitation from 1950 to 2012. Year 1 in the illustrative data corresponds to year 1950 in the observational data. Coloured lines represent changes over different 45 year periods indexed by their central year. Note that although DJF has 90 or 91 days, only days with non-zero rainfall are included which means that the number of data points included can be significantly fewer. The illustrative case in figure 1 is therefore an optimistic scenario in terms of data sample size.

For figure 3 the process underlying figure 2 was repeated for all E-Obs grid boxes in the European domain. The smallest change of consistent sign (identified from the ten evaluations at the given threshold and gridbox) is plotted. The availability of a gridded dataset facilitates this analysis but assumptions made in the interpolation procedure generate their own uncertainties [29, 30] and the varying density of the underlying station data means that some regions of figure 3 are more reliable than others. In the provision of climate services this should be assessed with respect to the particular data of interest to specific users. A programme of work repeating this analysis with reanalysis data, or even better, station data, would increase confidence in specific aspects of the results but would not be expected to change the general messages highlighted herein.

## References

- [1] CIBSE 2005 *TM36 Climate Change and the Indoor Environment: Impacts and Adaptation* (London: CIBSE)
- [2] Porter J R and Semenov M A 2005 Crop responses to climatic variation *Phil. Trans. R. Soc. B* **360** 2021–35
- [3] Milly P C D *et al* 2008 Stationarity is dead: whither water management? *Science* **319** 573–4
- [4] Hsiang S M 2010 Temperatures and cyclones strongly associated with economic production in the Caribbean and Central America *Proc. Natl Acad. Sci. USA* **107** 15367–72
- [5] Watanabe M *et al* 2014 Contribution of natural decadal variability to global warming acceleration and hiatus *Nat. Clim. Change* **4** 893–7
- [6] Chapman S C, Stainforth D A and Watkins N W 2013 On estimating local long term climate trends *Phil. Trans. R. Soc. A* **371** 20120287
- [7] Stainforth D A, Chapman S C and Watkins N W 2013 Mapping climate change in European temperature distributions *Environ. Res. Lett.* **8** 034031
- [8] Daron J D and Stainforth D A 2013 On predicting climate under climate change *Environ. Res. Lett.* **8** 034021
- [9] Reich B J 2012 Spatiotemporal quantile regression for detecting distributional changes in environmental processes *J. R. Stat. Soc. Ser. C* **61** 535–53
- [10] Morak S, Hegerl G C and Kenyon J 2011 Detectable regional changes in the number of warm nights *Geophys. Res. Lett.* **38** L17703
- [11] Christidis N, Jones G S and Stott P A 2015 Dramatically increasing chance of extremely hot summers since the 2003 European heatwave *Nat. Clim. Change* **5** 46–50
- [12] IPCC 2013 *Climate Change 2013: The Physical Science Basis. Contribution of Working Group I to the Fifth Assessment Report of the Intergovernmental Panel on Climate Change* (Cambridge: Cambridge University Press)
- [13] Stainforth D A, Allen M R, Tredger E R and Smith L A 2007 Confidence, uncertainty and decision-support relevance in climate predictions *Phil. Trans. R. Soc. A* **365** 2145–61
- [14] Collier J C, Bowman K P and North G R 2004 A comparison of tropical precipitation simulated by the community climate model with that measured by the tropical rainfall measuring mission satellite *J. Clim.* **17** 3319–33
- [15] van Oldenborgh G J *et al* 2009 Western Europe is warming much faster than expected *Clim. Past* **5** 1–12
- [16] New M, Hulme M and Jones P 2000 Representing twentieth-century space–time climate variability: II. Development of 1901–96 monthly grids of terrestrial surface climate *J. Clim.* **13** 2217–38
- [17] IPCC 2012 *Managing the Risks of Extreme Events and Disasters to Advance Climate Change Adaptation. A Special Report of Working Groups I and II of the Intergovernmental Panel on Climate Change* (Cambridge: Cambridge University Press)
- [18] Alexander L V *et al* 2006 Global observed changes in daily climate extremes of temperature and precipitation *J. Geophys. Res.-Atmos.* **111** D05109
- [19] Climdex 2015 *Datasets for Indices of Climate Extremes* (<http://climdex.org/indices.html>)
- [20] Wilby R L and Wigley T M L 2002 Future changes in the distribution of daily precipitation totals across North America *Geophys. Res. Lett.* **29** 39–1–4
- [21] Meehl G A *et al* 2009 Decadal prediction can it be skillful? *Bull. Amer. Meteorol. Soc.* **90** 1467
- [22] Groisman P Y and Easterling D R 1994 Variability and trends of total precipitation and snowfall over the United-States and Canada *J. Clim.* **7** 184–205
- [23] Groisman P Y *et al* 1999 Changes in the probability of heavy precipitation: Important indicators of climatic change *Clim. Change* **42** 243–83
- [24] van Oldenborgh G J, Haarsma R, de Vries H and Allen M R 2014 Cold extremes in North America versus mild weather in Europe: the winter 2013/2014 in the context of a warming world *Bull. Amer. Meteorol. Soc.* **96** 707–14
- [25] Stainforth D A, Downing T E, Washington R, Lopez A and New M 2007 Issues in the interpretation of climate model ensembles to inform decisions *Phil. Trans. R. Soc. A* **365** 2163–77
- [26] Haylock M R *et al* 2008 A European daily high-resolution gridded data set of surface temperature and precipitation for 1950–2006 *J. Geophys. Res.-Atmos.* **113** D20119
- [27] WMO 2011 *Climate Knowledge for Action: A Global Framework for Climate Services—Empowering the Most Vulnerable* (Geneva: World Meteorological Organisation)
- [28] Hazeleger W *et al* 2015 Tales of future weather *Nat. Clim. Change* **5** 107–13
- [29] Hofstra N, New M and McSweeney C 2010 The influence of interpolation and station network density on the distributions and trends of climate variables in gridded daily data *Clim. Dyn.* **35** 841–58
- [30] Hofstra N, Haylock M, New M and Jones P D 2009 Testing E-OBS European high-resolution gridded data set of daily precipitation and surface temperature *J. Geophys. Res.-Atmos.* **114** D21101